

Effects of Thermal Radiation on Magnetohydrodynamic (MHD) Flow of a Micropolar Fluid towards a Stagnation Point on a Vertical Plate

Olanrewaju, P.O.

Okedayo, G. T.

Gbadeyan, J. A.

Department of Mathematics

Covenant University

Ota, Nigeria, West Africa.

Abstract

The steady MHD mixed convection stagnation point flow towards a vertical surface immersed in an incompressible micropolar fluid in the presence of thermal radiation is investigated. The external velocity impinges normal to the wall and the wall temperature is assumed to vary linearly with the distance from the stagnation point. The governing partial differential equations are transformed into a system of ordinary differential equations, which is then solved numerically due to nonlinearity of the system by a shooting technique alongside with sixth order Runge-Kutta iteration scheme. The features of the flow and heat transfer characteristics for different values of the embedded flow parameters are analyzed and discussed. Both assisting and opposing flows are considered. We made comparison with Ishak et al [1] upper solution being the only stable solution in the absence of radiation and there were perfect agreement. The heat transfer rate and the skin friction were discussed extensively.

Keywords: Heat transfer; MHD; Micropolar fluid; Thermal radiation; Stagnation flow

1. Introduction

Micropolar fluids are fluid with microstructure. They belong to a class of fluids with nonsymmetric stress tensor that we shall call polar fluids. Micropolar fluids may also represent fluids consisting of rigid, randomly oriented (or spherical) particles suspended in a viscous medium, where the deformation of the particle is ignored. This constitutes a substantial generalization of the Navier-Stokes model and opens a new field of potential applications. The attractiveness and power of the model of micropolar fluids come from the fact that it is both a significant and a simple generalization of the classical Navier-Stokes model. The theory of micropolar fluids developed by Eringen [1,2] and has been a field of very active research for the last few decades as this class of fluids represents, mathematically, many industrial important fluids such as paints, body fluids, polymers, colloidal fluids, suspension fluids, animal blood, liquid crystal, etc among the various non-Newtonian fluids model. In addition to its classical velocity field, involve three gyration vectors. These latter degrees of freedom provide the necessary instrument to account for the intrinsic rotary motions and stretch of the local fluid elements. The theory of micropolar fluids [3] is a special case of the theory of simple microfluids.

This theory may have applications in the understanding of nemotogenic and smectogenic liquid crystals, flow of colloidal fluids, fluids with additives, suspension solutions, blood flows, fluids with bar like elements etc. Interesting aspects of theory and applications of micropolar fluids are dealt in the books by Eringen [4] and Lukaszewicz [5]. Micropolar fluid mechanics has received attention of many researchers and a good list of references on the published papers for this fluid can be found in Eringen [4] and Ishak et al. [6]. However, the associated MHD problems have not received much attention until recently.

Considering the linear theory of micropolar viscoelasticity has been carried out by Eringen [7]. Nazar et al. [8] studied stagnation point flow of a micropolar fluid towards a stretching sheet. Ali and Hayat [9] considered the peristaltic flow of a micropolar fluid in an asymmetric channel. Moreover, Sajid et al. [10] examined the homotopy analysis for boundary layer flow of a micropolar fluid through a porous channel. MHD flow of a micropolar fluid near a stagnation-point towards a non-linear stretching surface was considered by Hat et al [11]. [12] Investigated the effects of an endoscope on peristaltic flow of a micropolar fluid and also Hayat et al. [13] examined mixed convection flow of a micropolar fluid over a non-linearly stretching sheet. More recently, Ishak et al. [14] investigated magnetohydrodynamic (MHD) flow of a micropolar fluid towards a stagnation point on a vertical surface.

The present paper considers a steady MHD flow towards a stagnation point on a vertical surface immersed in a micropolar fluid in the presence of thermal radiation which is an extension of Ishak et al. [14] work. Therefore, the objective of the present study is to investigate the influence of radiation and other embedded parameters in the flow model and also for assisting and opposing flow respectively.

2. Analysis

We consider the steady, two-dimensional flow of an incompressible electrically conducting micropolar fluid in the presence of thermal radiation near the stagnation point on a vertical heated plate. It is assumed that the velocity of the flow external to the boundary layer $U(x)$ and the temperature $T_w(x)$ of the plate are proportional to the distance x from the stagnation point, i.e. $U(x) = ax$ and $T_w(x) = T_\infty + bx$, where a and b are constants. A uniform magnetic field of strength B_0 is assumed to be applied in the positive y -direction normal to the plate. The magnetic Reynolds number of the flow is taken to be small enough so that the induced magnetic field is negligible. In addition heat radiation effects are included. Under these assumptions along with the Boussinesq and boundary layer approximation, the system of equations, which models the flow is given by

$$\frac{\partial u}{\partial x} + \frac{\partial v}{\partial y} = 0, \quad (1)$$

$$u \frac{\partial u}{\partial x} + v \frac{\partial u}{\partial y} = U \frac{dU}{dx} + \left(\frac{\mu + k}{\rho} \right) \frac{\partial^2 u}{\partial y^2} + \frac{k \partial N}{\rho \partial y} + \frac{\sigma B_0^2}{\rho} (U - u) + g\beta(T - T_\infty), \quad (2)$$

$$\rho j \left(u \frac{\partial N}{\partial x} + v \frac{\partial N}{\partial y} \right) = \gamma \frac{\partial^2 N}{\partial y^2} - k \left(2N + \frac{\partial u}{\partial y} \right), \quad (3)$$

$$u \frac{\partial T}{\partial x} + v \frac{\partial T}{\partial y} = \alpha \frac{\partial^2 T}{\partial y^2} - \frac{1}{c_p \rho} \frac{\partial q_r}{\partial y}, \quad (4)$$

subject to the boundary conditions

$$u = 0, \quad v = 0, \quad N = -\frac{1}{2} \frac{\partial u}{\partial y}, \quad T = T_w(x) \quad \text{at } y = 0, \quad (5)$$

$$u \rightarrow U(x), \quad N \rightarrow 0, \quad T \rightarrow T_\infty \quad \text{as } y \rightarrow \infty,$$

where u and v are the velocity components along the x - and y -axes, respectively, g is the acceleration due to gravity and T is the fluid temperature in the boundary layer. Furthermore, μ , k , ρ , β , j , N , γ , α , c_p and q_r are respectively the dynamic viscosity, vortex viscosity (or the microrotation viscosity), fluid density, thermal expansion coefficient, microinertial density, microrotation vector (or angular velocity), spin gradient viscosity, thermal diffusivity, specific heat at constant pressure and heat flux. We follow the work of many authors by assuming that $\gamma = (\mu + k/2)j = \mu(1 + K/2)j$, where $K = k/\mu$ is the material parameter. This assumption is involved to allow the field of equations predicts the correct behavior in the limiting case when the microstructure effects become negligible and the total spin N reduces to the angular velocity (see Ishak et al [14]). By the Rosseland approximation the radiative heat flux can be reduced in the form

$$q_r = -\frac{4\Gamma}{3k^*} \frac{\partial T^4}{\partial y}, \quad (6)$$

where Γ and k^* are the Stefan-Boltzmann constant and the mean absorption coefficient respectively. Invoking Taylor series, one has

$$T^4 \approx 4T_0^3 T - 3T_0^4, \quad (7)$$

where in the above equation T_0 is the temperature at the centre $y = 0$ and terms of higher order are neglected.

The continuity equation (1) is satisfied by introducing a stream function Ψ such that

$$u = \frac{\partial \Psi}{\partial y}, \quad v = -\frac{\partial \Psi}{\partial x}. \quad (8)$$

The momentum, angular momentum and energy equations can be transformed into the corresponding ordinary differential equations by the following substitutions:

$$\eta = \left(\frac{a}{\nu}\right)^{1/2} y, \quad f(\eta) = \frac{\psi}{(a\nu)^{1/2} x}, \quad h(\eta) = \frac{N}{a(a/\nu)^{1/2} x}, \quad \theta = \frac{T - T_\infty}{T_w - T_\infty}. \tag{9}$$

The transformed ordinary differential equations are :

$$(1 + K)f''' + ff'' + 1 - f'^2 + Kh' + M(1 - f') + \lambda\theta = 0, \tag{10}$$

$$\left(1 + \frac{K}{2}\right)h'' + fh' - f'h - K(2h + f'') = 0, \tag{11}$$

$$\left(1 + \frac{4Ra}{3}\right)\theta + Pr f\theta' - Pr f'\theta = 0, \tag{12}$$

subject to the boundary conditions (5) which become

$$f(0) = 0, \quad f'(0) = 0, \quad h(0) = -\frac{1}{2} f''(0), \quad \theta(0) = 1, \tag{13}$$

$$f'(\eta) \rightarrow 1, \quad h(\eta) \rightarrow 0, \quad \theta(\eta) \rightarrow 0 \text{ as } \eta \rightarrow \infty,$$

where we have $j = \nu/a$ as a characteristic length (see Rees and Bassom [10]). In the above equations, primes denote differentiation with respect to η , $Pr = \nu/\alpha$ is the Prandtl number, $M = B_0^2 \sigma / \rho a$ is the magnetic parameter, $\lambda = Gr_x / Re_x^2$ is the buoyancy or mixed convection parameter, $Ra = 4\alpha \Gamma T_\infty^3 / k^* \mu$ is the thermal radiation parameter, $Gr_x = g\beta(T_w - T_\infty)x^3 / \nu^2$ is the local Grashof number and $Re_x = Ux/\nu$ is the local Reynolds number. We further notice that λ is a constant with $\lambda < 0$ and $\lambda > 0$ correspond to the opposing and assisting flows, respectively, while $\lambda = 0$ (i.e. $T_w = T_\infty$) is purely a forced convection flow. When $M = 0$, and $Ra = 0$, the problem reduces to those considered by Lol et al. [16], while when $M = 0$, $Ra = 0$ and $K = 0$ it reduces to those of Ramachandran et al. [15]. Similarly, when $Ra = 0$, the problem reduces to those of Ishak et al [14].

Table 1: Values of $f''(0)$ for different values of Pr when $M = 0, K = 0, \lambda = 1$, and $Ra = 0$

Pr	Ramachandran et al. [15]	Lok et al. [16]	Ishak et al. [14]	Present result
0.7	1.7063	1.706376	1.7063	1.70632271203751262
1	-	-	1.6755	1.67543657183886084
7	1.5179	1.517952	1.5179	1.51791261937622068
10	-	-	1.4928	1.49283867303847640

Table 2: Values of $-\theta'(0)$ for different values of Pr when $M = 0, K = 0, \lambda = 1$, and $Ra = 0$

Pr	Ramachandran et al. [15]	Lok et al. [16]	Ishak et al. [14]	Present result
0.7	0.7641	0.764087	0.7641	0.764063401496150818
1	-	-	0.8708	0.870778601174578282
7	1.7224	1.722775	1.7225	1.722381606491674150
10	-	-	1.9448	1.94461739662861999

Table 3: Values of $H(0), -\theta(0)$ and $f''(0)$ for the embedded flow parameters in the flow model

Pr	M	K	λ	Ra	$H(0)$	$-\theta'(0)$	$f''(0)$
0.7	1	1	1	1	0.673533225654727397	0.540053877956969353	1.61468454020605878
1	1	1	1	1	-0.79738035280778796	0.619939494830565318	1.59476070561557592
7	1	1	1	1	-0.74378966234346344	1.264867553643981301	1.48757932468692688
10	1	1	1	1	-0.73490475392458787	1.433965306315825302	1.46980950784917576
1	2	1	1	1	-0.88888840182570960	0.631755666137700955	1.77777680365141922
1	3	1	1	1	-0.97033677598117162	0.641134514774587827	1.94067355196234326
1	4	1	1	1	-1.04444566276134274	0.648879550533652982	2.08889132552268552
1	1	2	1	1	-0.68178153667736074	0.599054824397862728	1.36356307335472148
1	1	3	1	1	-0.60520930794100857	0.582757691664827826	1.21041861588201716
1	1	1	-2	1	0.111572066457112887	-0.18701355600946964	-0.22314413291422576
1	1	1	-1	1	-0.46737800347075114	0.547042658498067990	0.934756006941502294
1	1	1	2	1	-0.94762472078923587	0.648299389679389604	1.895249441578471744
1	1	1	3	1	-1.09113677810678422	0.673338127653544505	2.18227355621356844
1	1	1	1	2	-0.80996660438664480	0.520263351040158972	1.61993320877328961
1	1	1	1	3	-0.81835396288089890	0.460085611836912378	1.63670792576179780
1	1	1	1	4	-0.82455436995093500	0.418308462705216100	1.64910873990187002
1	1	1	1	0	-0.77342489869876796	0.851744190841606907	1.54684979739753592

Table 4: Values of $f''(0)$ and $-\theta'(0)$ for $Pr = 1, M = 1, K = 0$ and 1 , and for various values of λ

Pr	M	K	Ra	λ	$f''(0)$	$-\theta'(0)$
1	1	0	1	-3	-0.67712667258229630	0.0666358397658931984
1	1	0	1	-2	-0.23535322015789078	-0.17232126269374437
1	1	0	1	-1	1.11480374634655521	0.567019781207243834
1	1	0	1	0	1.58533069663939318	0.612177070698151304
1	1	0	1	1	2.02205641484308174	0.649007910757433470
1	1	0	1	2	2.43470273998483844	0.680445476704595986
1	1	1	1	-3	-0.52821696260852701	0.0284101877934617754
1	1	1	1	-2	-0.22373720258648052	-0.187500142451099864
1	1	1	1	-1	0.93475600766665134	0.547042659772633110
1	1	1	1	0	1.27684219627811402	0.586967357231851006
1	1	1	1	1	1.59476070545589454	0.619939495091724744
1	1	1	1	2	1.89524944139703820	0.648299389820970796

The physical quantities of interest are the skin friction coefficient C_f and the local Nusselt number Nu_x , which are defined as

$$C_f = \frac{\tau_w}{\rho U^2 / 2}, \quad Nu_x = \frac{xq_w}{k(T_w - T_\infty)}, \tag{14}$$

Where the wall shear stress τ_w and the heat flux q_w are given by

$$\tau_w = ([\mu + k] \frac{\partial u}{\partial y} + kN)_{y=0}, \quad q_w = -k \left(\frac{\partial T}{\partial y} \right)_{y=0}, \tag{15}$$

With k being the thermal conductivity. Using the similarity variables (9), we have

$$\frac{1}{2} C_f Re_x^{1/2} = \left(1 + \frac{K}{2} \right) f''(0), \quad \frac{Nu_x}{Re_x^{1/2}} = -\theta'(0), \tag{16}$$

which have been computed in tables 3 and 4.

3. Results and discussion

Eqs. (8)-(10) constitute a highly non-linear coupled boundary value problem of third and second-order. So we develop most effective numerical shooting technique with sixth-order Runge-Kutta integration algorithm. To select η_∞ we begin with some initial guess value and solve the problem with some particular set of parameters to obtain $H(0), f''(0)$ and $\theta'(0)$.

The solution process is repeated with another larger value of η_∞ until two successive values of $H(0), f''(0)$ and $\theta'(0)$ differ only after desired digit signifying the limit of the boundary along η . The last value of η_∞ is chosen as appropriate value for that particular simultaneous equations of first order for seven unknowns following the method of superposition. To solve this system we require seven initial conditions whilst we have only two initial conditions $f'(0)$ and $f(0)$ on f , two initial conditions on each on θ and H . Still there are three initial conditions $f''(0), \theta'(0)$ and $H(0)$ which are not prescribed. Now, we employ numerical shooting technique where these two ending boundary conditions are utilized to produce two unknown initial conditions at $\eta = 0$. In this calculation, the step size $\Delta\eta=0.001$ is used while obtaining the numerical solution with $\eta_{\max}=11$ and five-decimal accuracy as the criterion for convergence.

Numerical calculations have been carried out for different values of the thermophysical parameters controlling the fluid dynamics in the flow regime. Tables (1) and (2) show the comparison of Ramachandran et al. [15], Lok et al. [16] and Ishak et al [14] works with the present work for $M = 0, K = 0, \lambda = 0, Ra = 0$ and for various values of Prandtl numbers Pr and it is noteworthy that there is a excellent agreement. From table (3), it is seen that the local skin friction together with the heat transfer rate at the moving plate surface increases with increasing magnetic field parameter while the angular velocity at the surface decreases. The rate of heat transfer and the local skin friction at the plate surface decreases with increasing the material parameter K while the angular velocity at the surface increases. The Nusselt number and the local Skin friction at the wall surface increases with an increase in the convection parameter λ for opposing and assisting flows. It was clearly seen that increasing the thermal radiation parameter decreases the heat transfer rate at the wall surface and increasing the local Skin friction at the wall surface. This table shows that there is a favorable pressure gradient due to the buoyancy forces, which results in the flow being accelerated and consequently there is a larger skin friction coefficient than in the non-buoyancy case ($\lambda = 0$). In table (4), we computed the local Skin friction and heat transfer rate at the surface for $Pr = 1, M = 1, k = 0, I$ and for various values of convection parameter λ . For $K = 0$ and I , the heat transfer rate and the local Skin friction at the surface increases which agrees with figs. (8) and (9) in Ishak et al. [14] work.

The velocity, angular velocity and temperature profiles as shown in Figs. 1-13. Figs. 1-5 represent the velocity profiles for the embedded flow parameters. It is clearly seen that increasing in M, Pr, K and Ra decreases the velocity boundary layer thickness even for both opposing and assisting flows (see figs. 1-5). Figs. 6-9 represent the angular velocity profiles for the flow parameters. The effects of all the embedded flow parameters have great influence on the angular velocity boundary layer thickness for both assisting and opposing flows. The influence of the embedded flow parameters on the temperature field is represented by figs. 10-13. Increasing the Prandtl number Pr decreases the thermal boundary layer thickness across the plate which agrees with literatures (see fig. 10). Other parameters like the material parameter K and the radiation parameter increases the thermal boundary layer thickness as they increased.

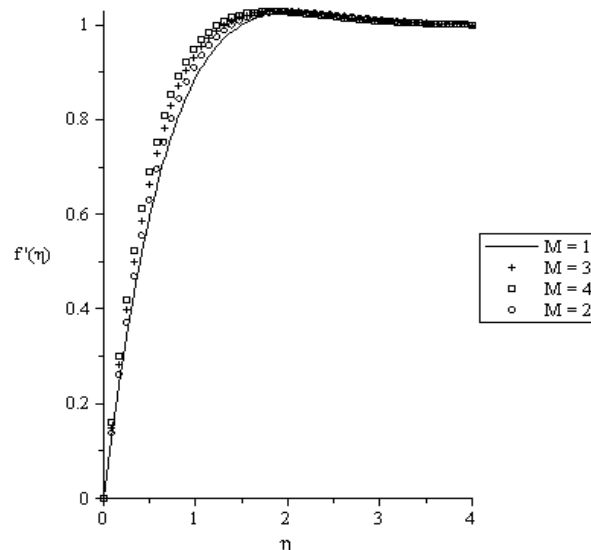


Figure 1: Velocity profiles for $Pr = 0.72, K = 1, \lambda = 1, Ra = 1$

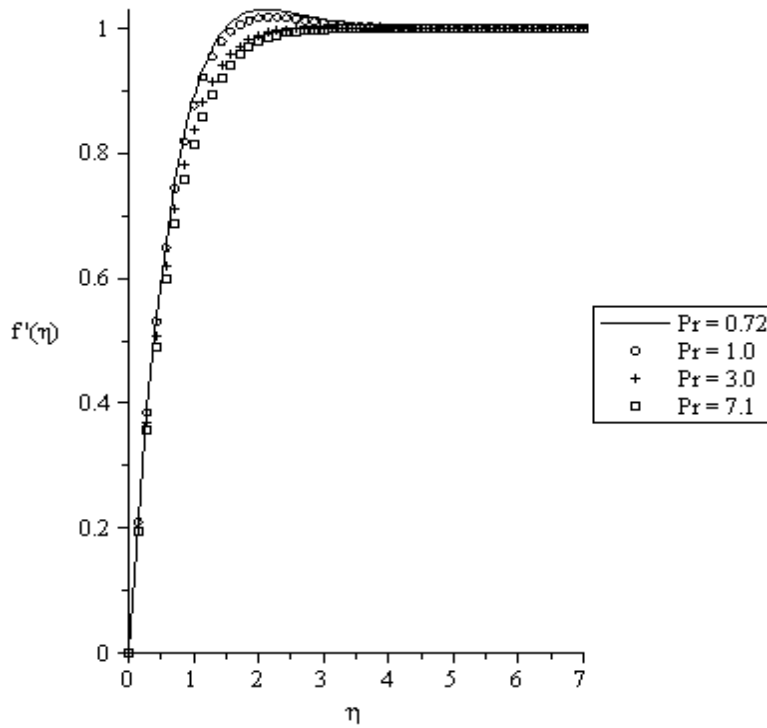


Figure 2: Velocity profiles for $M = 1, K = 1, \lambda = 1, Ra = 1$

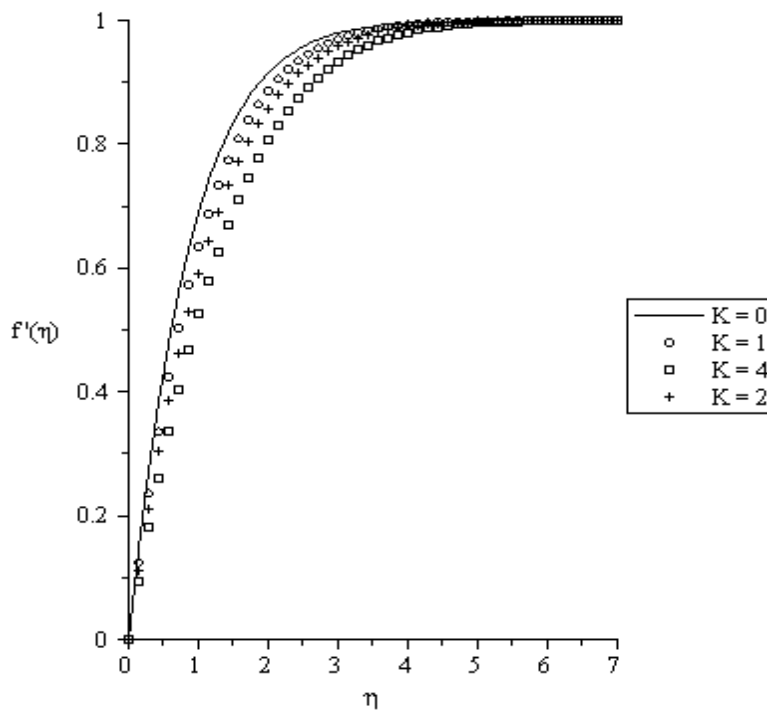


Figure 3: Velocity profiles for $M = 1, Pr = 0.72, \lambda = -1, Ra = 1$ (opposing flow)

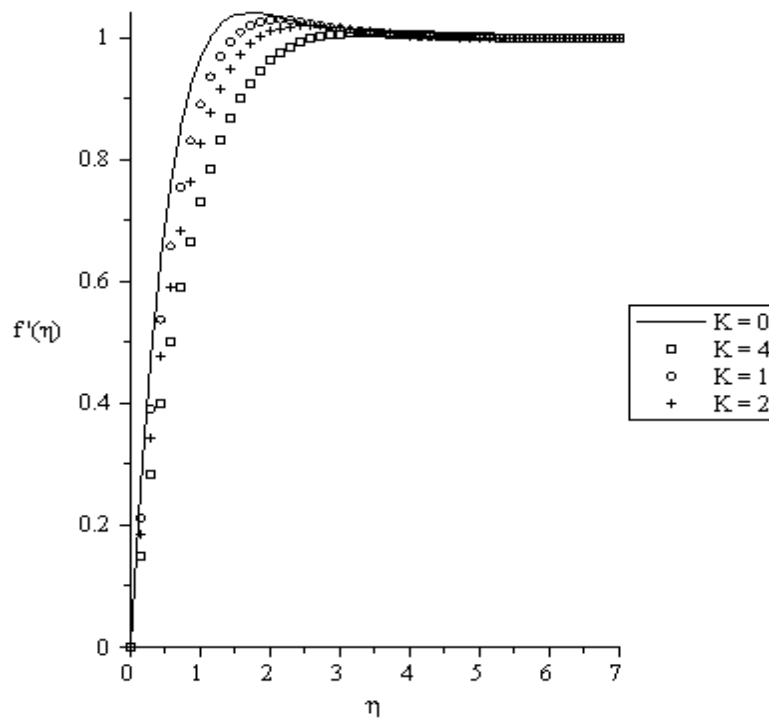


Figure 4: Velocity profiles for $M = 1, Pr = 0.72, \lambda = 1, Ra = 1$ (assisting flow)

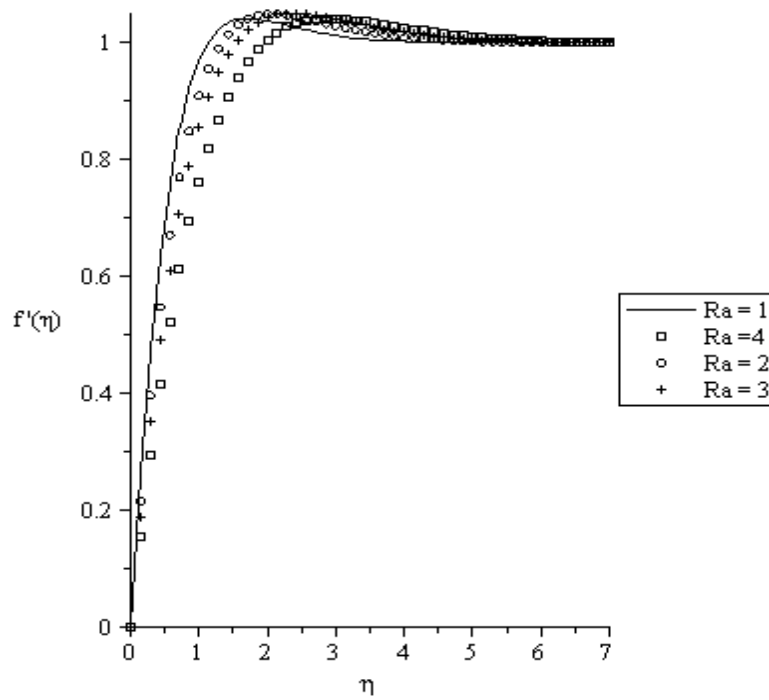


Figure 5: Velocity profiles for $M = 1, Pr = 0.72, \lambda = 1, K = 1$

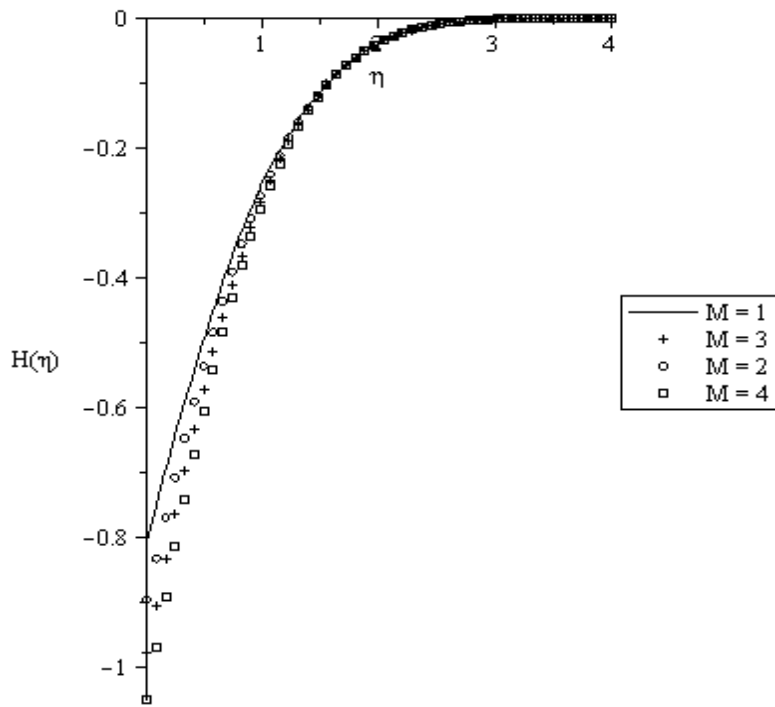


Figure 6: Angular Velocity profiles for $Pr = 0.72$, $K = 1$, $\lambda = 1$, $Ra = 1$

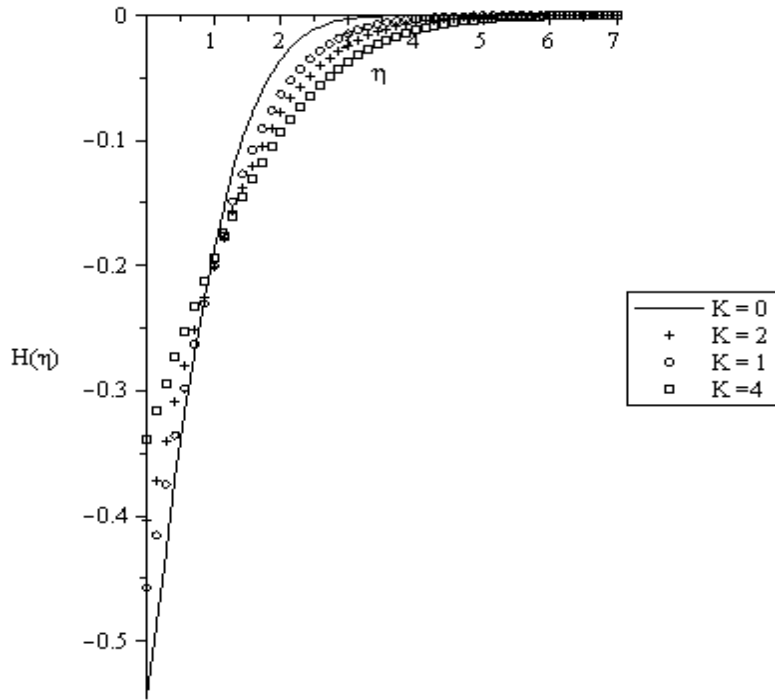


Figure 7: Angular Velocity profiles for $M = 1$, $Pr = 0.72$, $\lambda = -1$, $Ra = 1$ (opposing flow)

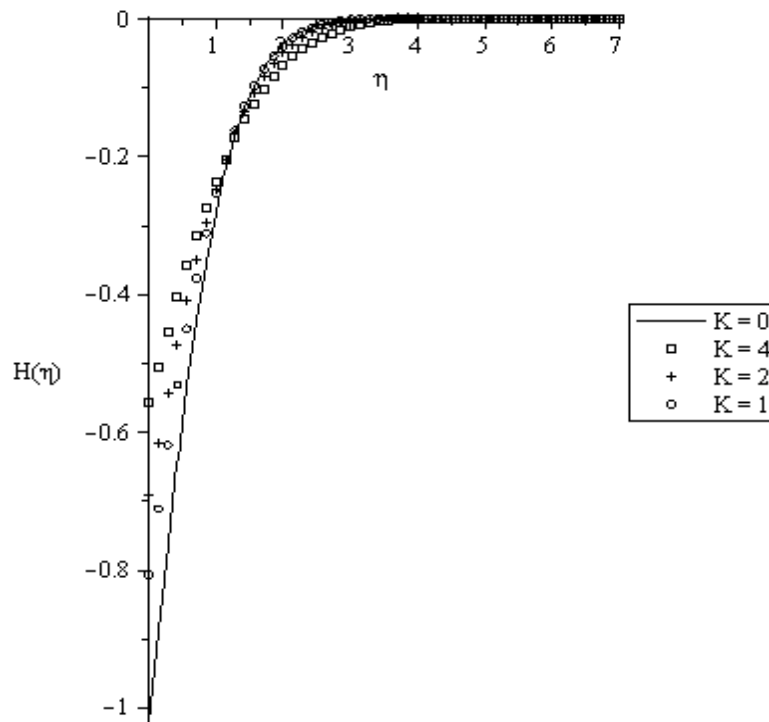


Figure 8: Angular Velocity profiles for $M = 1, Pr = 0.72, \lambda = 1, Ra = 1$ (assisting flow)

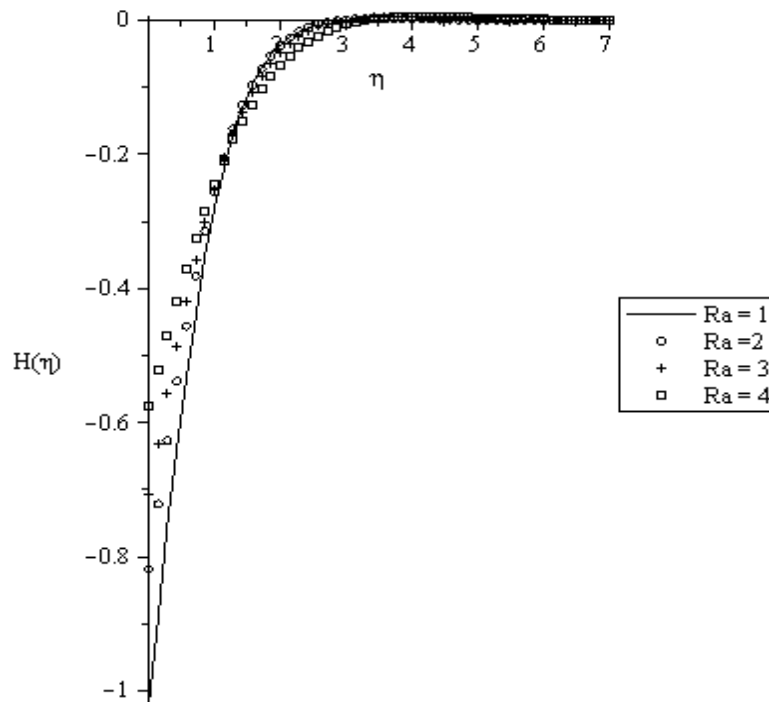


Figure 9: Angular Velocity profiles for $M = 1, Pr = 0.72, \lambda = 1, K = 1$

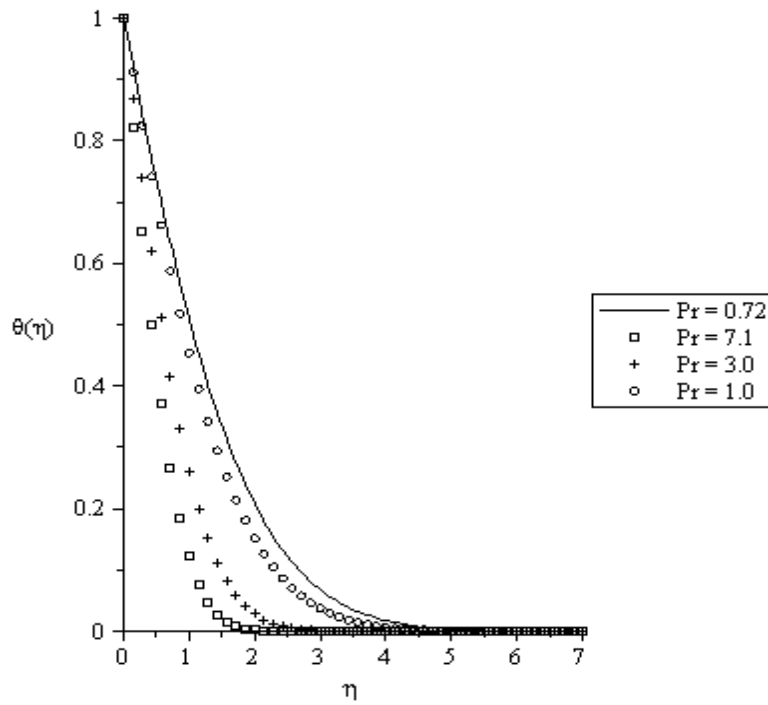


Figure 10: Temperature profiles for $M = 1, K = 1, \lambda = 1, Ra = 1$

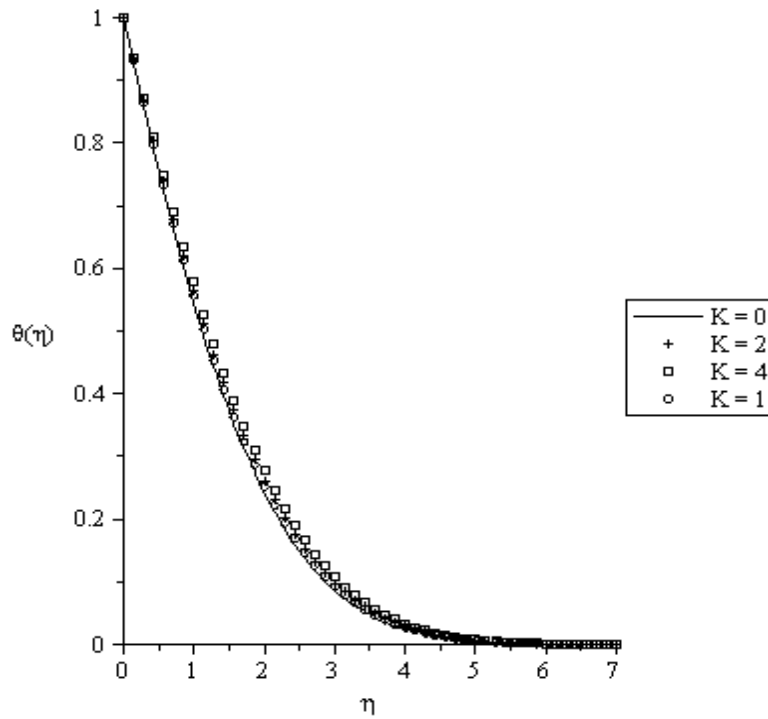


Figure 11: Temperature profiles for $M = 1, Pr = 0.72, \lambda = -1, Ra = 1$ (opposing flow)

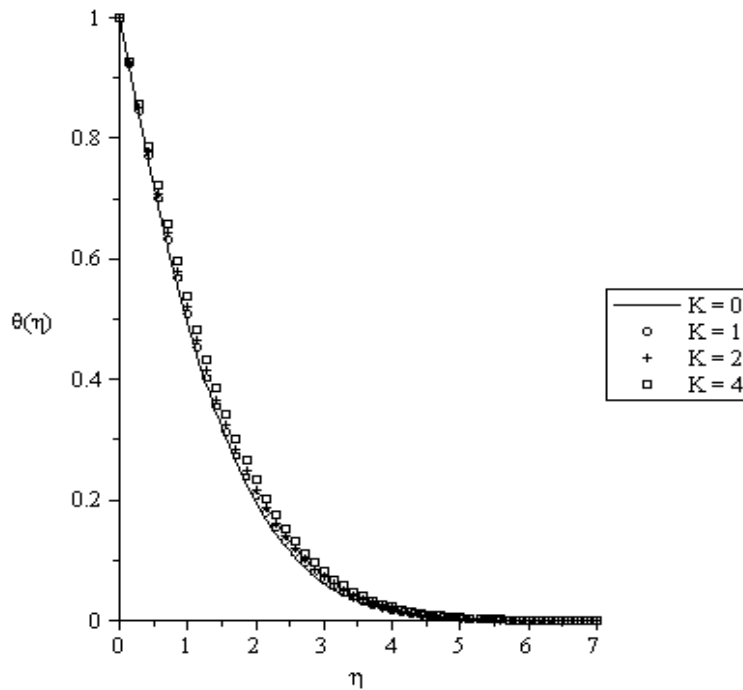


Figure 12: Temperature profiles for $M = 1, Pr = 0.72, \lambda = 1, Ra = 1$ (assisting flow)

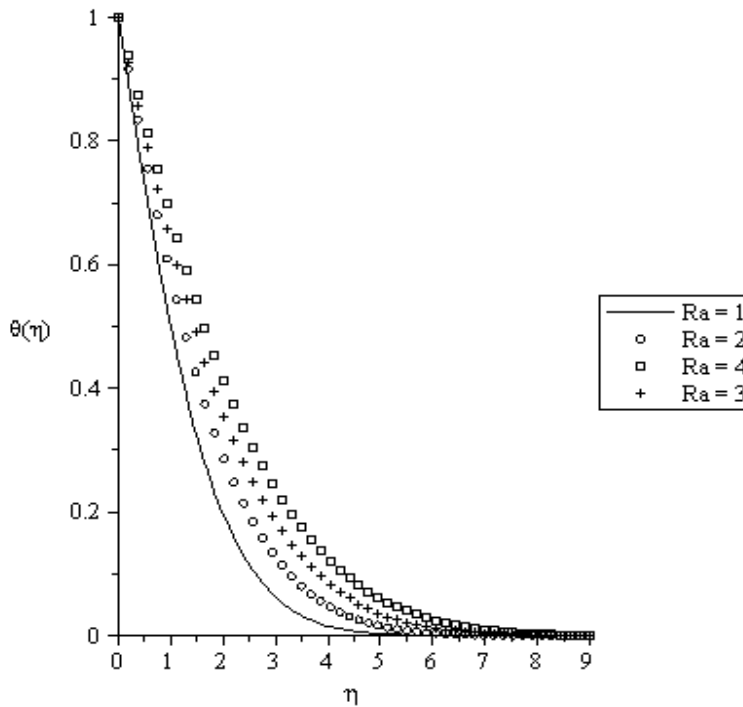


Figure 13: Temperature profiles for $M = 1, Pr = 0.72, \lambda = 1, K = 1$

4. Conclusions

We have theoretically investigated the similarity solutions for the steady MHD flow towards a stagnation point on a vertical immersed in an incompressible micropolar fluid with thermal radiation. The transformed non-linear ordinary differential equations were solved numerically using shooting method with sixth order of Runge-Kutta integration technique. There was an existence of reversed flow in the assisting flow regime also. Thermal radiation absorption has a greater influence on the velocity, angular velocity and temperature fields, thus micropolar fluid delays the boundary layer separation, which in turn increases the range of similarity solutions compared to Newtonian fluid.

Therefore, from the above analysis we could conclude that for micropolar fluids flow, the radiation effects play a significant role and should not be neglected.

Acknowledgements

POO would like to thank Covenant University, Ota, Nigeria, West Africa for their financial support for the research work.

References

- [1] A.C. Eringen, Theory of micropolar fluids, *J. Math. Mech.* 16 (1966) 1-18.
- [2] A.C. Eringen, Theory of thermomicropolar fluids, *J. Math. Anal. Appl.* 38 (1972) 480-496.
- [3] A.C. Eringen, Simple microfluids, *Int. J. Eng. Sci.* 2 (1964) 205-217.
- [4] A.C. Eringen, *Microcontinuum Field Theories II: Fluent Media*, Springer, New York, 2001.
- [5] G. Lukaszewicz, *Micropolar Fluids: Theory and Applications*, Birkhauser, Basel, 1999.
- [6] A. Ishak, R. Nazar, I. Pop, Moving wedge and flat plate in a micropolar fluid, *Int. J. Eng. Sci.* 44 (2006) 1225-1236.
- [7] A.C. Eringen, Linear theory of micropolar viscoelasticity, *Int. J. Eng. Sci.* 5, issues 2 (1967) 191-204.
- [8] R. Nazar, N. Amin, D. Filip, I. Pop, Stagnation point flow of a micropolar fluid towards a stretching sheet, *Int. J. of Non-Linear Mechanics*, 39, Issue 7 (2004) 1227-1235.
- [9] N. Ali, T. Hayat, Peristaltic flow of a micropolar fluid in an asymmetric channel, *Computer & Mathematics with Applications*, 55, Issue 4 (2008) 589-608.
- [10] M. Sajid, Z. Abbas, T. Hayat, Homotopy analysis for boundary layer flow of a micropolar fluid through a porous channel, *Applied Mathematical Modelling*, 33, Issue 11 (2009) 4120-4125.
- [11] T. Hayat, T. Javed, Z. Abbas, MHD flow of a micropolar fluid near a stagnation-point towards a non-linear stretching surface, *Nonlinear Analysis: Real World Applications*, 10, Issue 3 (2009) 1514-1526 .
- [12] T. Hayat, N. Ali, Effects of an endoscope on peristaltic of a micropolar fluid, *Mathematical and Computer Modelling*, 48, Issue 5-6 (2008) 721-733.
- [13] T. Hayat, Z. Abbas, T. Javed, Mixed convection flow of a micropolar fluid over a non-linearly stretching sheet, *Physics Letters A*, 372, Issue 5 (2008) 637-647.
- [14] A. Ishak, R. Nazar, I. Pop, Magneto-hydrodynamics (MHD) flow of a micropolar fluid towards a stagnation point on a vertical surface, *Computers and Mathematics with Applications* 56 (2008) 3188-3194.
- [15] N. Ramachandran, T.S. Chem, B.F. Armaly, Mixed convection in a stagnation flows adjacent to a vertical surfaces, *ASME J. Heat Mass Transfer* 110 (1988) 373-377.
- [16] Y.Y. Lok, N. Amin, D. Campean, I. Pop, Steady mixed convection flow of a micropolar fluid near the stagnation point on a vertical surface, *Int. J. Numerical Methods Heat Flow* 15 (2005) 654-670.